

## High Temperature Resistant Silane/Zirconium-Oxocluster Hybrid Copolymers Containing “Free” Thiol/Ene Functionalities in the Polymer Matrix

Simona Maggini, Elisa Cappelletto, Rosa Di Maggio

Dipartimento di Ingegneria dei Materiali e Tecnologie Industriali, Università degli Studi di Trento, Trento 38123, Italy

Correspondence to: S. Maggini (E-mail: simona.maggini.unitn.it or simonamaggini@gmail.com)

**ABSTRACT:** Inorganic–organic hybrid copolymers are promising materials where the size of the inorganic/organic domains, the phase continuity and the interface between the domains play an important role in their behavior. Two types of hybrid copolymers composed of 3-butyrate-substituted zirconium-oxoclusters covalently bonded to a (3-mercaptopropyl)trimethoxysilane or a vinyltrimethoxysilane matrix are investigated in bulk. Their properties are directly correlated with the degree of condensation of the silanes and the alkyne-3-mercaptopropyl or alkyne-vinyl interface. Both copolymers show storage moduli and glass-transition temperatures ( $T_{gG'}$ ) above 130 MPa and 230°C. However, the more impressive results are achieved with the (3-mercaptopropyl)trimethoxysilane copolymer where a  $T_{gG'}$  of about 300°C holds over six dynamical mechanical spectroscopy analyses. In addition to their excellent thermo-mechanical properties, the copolymers show unreacted 3-mercaptopropyl or vinyl groups which could be employed either in direct usage of the materials or for post-functional modifications. © 2012 Wiley Periodicals, Inc. *J. Appl. Polym. Sci.* 000: 000–000, 2012

**KEYWORDS:** thermal properties; nanostructured polymers; functionalization of polymers; stimuli-sensitive polymers; photopolymerization

Received 1 March 2012; accepted 22 April 2012; published online

DOI: 10.1002/app.37940

### INTRODUCTION

Hybrid materials composed of inorganic and organic building blocks have shown very interesting characteristics that are not found in organic polymers or inorganic materials alone. In particular, the preparation of hybrid materials through the use of preformed organically modified metal-oxoclusters is a relatively untapped direction but has already resulted in coatings with appealing thermo-mechanical properties.<sup>1–3</sup> The modified metal-oxoclusters organize the polymer architecture and, when grafted to the polymer matrix through covalent bonds, retain a uniform distribution.

Inorganic–organic (i/o) hybrid coatings and bulk materials containing the vinylacetate-substituted zirconium-oxocluster  $[\text{Zr}_6\text{O}_4(\text{O}-\text{H})_4(\text{OOCCH}_2\text{CH}=\text{CH}_2)_{12}(n\text{-PrOH})_2 \cdot 4(\text{CH}_2=\text{CHCH}_2\text{COOH})]$  ( $\text{Zr}_{12}$ ) polymerized with monomers with ene functional groups have shown transparency, hydrophobicity, and high thermo-mechanical and chemical stability.<sup>4–7</sup> When the monomer is a silane, the structural chemical bonds are formed through the condensation of the silanes and the radical polymerization of the vinylacetate ligands with the ene functional groups of the silanes. The properties of the material are closely

correlated with the degree of condensation (DC) of the silanes and the type of vinylacetate-substituted zirconium-oxoclusters/silanes interface. In this article, i/o hybrid copolymers composed of the 3-butyrate-substituted zirconium-oxoclusters  $[\text{Zr}_6\text{O}_4(\text{O}-\text{H})_4(\text{OOCCH}_2\text{C}\equiv\text{CH})_{12}]_2$  ( $\text{Zr}_6$ ) and vinyltrimethoxysilane (VTMS) or (3-mercaptopropyl)trimethoxysilane (MPTMS) monomers are considered to evaluate the increased reticulation of the polymer matrix given by the alkyne and to compare the effect of the different zirconium-oxocluster/silane interfaces on the final properties of the materials. The MPTMS monomer was selected to take advantage of the thiol-alkyne polymerization which offers high conversion rates, selectivity, modularity, insensitivity to oxygen inhibition, and the possibility of photo-initiation.<sup>8–12</sup> Moreover, the thiol functional groups change the hydrophobic nature of the copolymer and could be of interest for future applications as paper coatings since it is known to help to inhibit the yellowing of paper through its antioxidant behaviors.<sup>13–16</sup>

The copolymers were prepared through a sol–gel process without organosilane pre-hydrolysis. The absence of pre-hydrolysis was justified by previous studies,<sup>5,6</sup> which showed how the pre-

© 2012 Wiley Periodicals, Inc.

hydrolysis leads to a larger phase separation between the siloxane network and the zirconia domains.

The characterization and the thermo-mechanical studies of the copolymers were carried out by using fourier transform infrared (FTIR), nuclear magnetic resonance ( $^{29}\text{Si}$ ,  $^{13}\text{C}$ , and  $^1\text{H}$ -NMR) and dynamical mechanical spectroscopy (DMS), thermogravimetry (TGA), and differential scanning calorimetry (DSC). All the copolymers showed transparency, high stiffness and high glass-transition temperatures in the absence of remarkable mass loss and shrinkage. The copolymers can be successfully produced in bulk form or as a thin film. Here, their performance in bulk is described. A separate work describes their application in thin film as a protective coating for paper.

## EXPERIMENTAL

### Instrumentation

DSC analyses were performed using a DSC92 SETARAM, from 30°C to 200°C in nitrogen with a heating rate of 10°C/min.

Thermogravimetric analysis (TGA) was performed from 30°C to 1000°C in argon and in air with a heating rate of 10°C/min, using a Labsys SETARAM thermobalance.

FTIR was recorded in reflectance mode (ATR system with a zinc selenide crystal) in the range 4000–650  $\text{cm}^{-1}$ , using a PerkinElmer Spectrum One instrument. The spectra were recorded with a resolution of 2  $\text{cm}^{-1}$  with each spectra averaged over 64 scans. The intensity and the type of peak vibrations are indicated by the following abbreviations: w = weak, m = medium, s = strong,  $\nu_{\text{stretch}}$  = stretching,  $\nu_{\text{bend}}$  = bending,  $\nu_{\text{as}}$  = asymmetric,  $\nu_{\text{s}}$  = symmetric.

Solid state NMR analyses were carried out with a Bruker AVANCE 400 WB instrument, for  $^1\text{H}$  (400.13 MHz),  $^{29}\text{Si}$  (79.50 MHz) and  $^{13}\text{C}$  (100.61 MHz) experiments. Chemical shifts are quoted in parts per million (ppm). Samples were packed in 4 mm-zirconia rotors, which were spun at 9.0 kHz under air flow for  $^{29}\text{Si}$  and  $^{13}\text{C}$  analyses, and at 11 kHz for  $^1\text{H}$  analyses. The conventional  $T^n$  notation, where  $T$  represents a silicon atom and  $n$  the number of bridging oxygen atoms per silicon, was used to describe the  $^{29}\text{Si}$  spectra. According to this notation  $T^0$  represented the starting alkoxy silane. The relative amount of  $T^1$ ,  $T^2$ , and  $T^3$  species were determined by integration of the NMR spectra. The DC was defined as  $\text{DC} = \sum_n nT^n/f$ , where  $f$  is the functionality of the precursor; for VTMS and MPTMS,  $f = 3$ .

ESEM scans were obtained using a Philips ESEM-TMP XL30 and the microanalysis was conducted using a Falcon-EDAX with a carbon-uranium detector connected to the microscope.

DMS was performed in shear mode using a Seiko DMS6100 instrument at a frequency of 1 Hz, with a linear displacement of 0.005 mm and initial applied force of 1000 mN. Storage modulus, loss modulus, and  $\tan \delta$  were measured in the temperature range of 30–300°C with heating rate of 10°C/min and in an air atmosphere. The measurements were performed on cylindrical samples.

### Materials

All commercial reagents and solvents employed were of high-grade purity and were used as supplied without further purifica-

tion. The anhydrous solvents: *n*-propanol 99.7% and tetrahydrofuran (THF)  $\geq 99.9\%$  were purchased from Sigma-Aldrich. The 3-butynoic acid and  $[\text{Zr}_6\text{O}_4(\text{OH})_4(\text{O}_2\text{CCH}_2\text{C}\equiv\text{CH})_{12}]$  were synthesized according the procedure in the literature.<sup>17</sup> All manipulations were performed under aerobic conditions unless standard Schlenk techniques were required.

### Synthesis of $[\text{Zr}_6\text{O}_4(\text{OH})_4(\text{O}_2\text{CCH}_2\text{C}\equiv\text{CH})_{12}]$ ( $\text{Zr}_6$ )

$\text{Zr}(\text{OPr}^n)_4$  at 70% (27.0 mL) was added to a solution of 3-butynoic acid (15.3 g) in anhydrous *n*-propanol (20.0 mL) under an inert atmosphere. The mixture was stirred vigorously at room temperature for 1 h. The solvent was evaporated and the residue washed with anhydrous *n*-propanol and diethyl ether. The precipitate was recovered by filtration and dried under vacuum. A cream colored solid was obtained (15.4 g).

### Synthesis of the $\text{Zr}_6/\text{VTMS}/\text{BPO}$ Copolymer

#### ( $\text{Zr} : \text{Si}$ molar ratio 1 : 10)

VTMS (114.0 mL) was added to a solution of  $[\text{Zr}_6\text{O}_4(\text{OH})_4(\text{O}_2\text{CCH}_2\text{C}\equiv\text{CH})_{12}]$  (20.9 g) in anhydrous THF (5.0 mL), then BPO (1 wt % of VTMS) was added and the mixture was stirred at room temperature for 2 h or until a clear solution was obtained.

For the preparation of the bulk specimen, the previous solution was evaporated to dryness, leaving a yellow transparent xerogel ( $\text{Zr}_6/\text{VTMS}/\text{BPO}$ ). The sample was heated at 90°C for 30 min. A cylindrical sample of length 3.28 mm and diameter 6.02 mm was produced. DMS analysis — after the 1st run:  $3.18 \times 5.86$  mm; 2nd run:  $2.85 \times 5.78$  mm.

$^1\text{H}$  NMR (400 MHz,  $\delta$ ): 5.8, 3.2;  $^{13}\text{C}$  NMR (100 MHz,  $\delta$ ): 223.0 (C=C=C), 217.7 (C=C=C), 214.3 (C=C=C), 172.0 (COO), 133.8 (=CH), 128.0 (=CH<sub>2</sub>), 88.6 (CH<sub>2</sub>-C=C=C), 75.9 (C=C=CH), 69.6 ( $\Xi\text{CH}$ ), 53.5 (CH<sub>2</sub>), 47.8 (OCH<sub>3</sub>), 39.6 (CH<sub>2</sub>), 25.8 (OOCCH<sub>2</sub>), 17.8 (CH<sub>2</sub>);  $^{29}\text{Si}$  NMR (79 MHz,  $\delta$ ): -62.9 [Si(OSi)], -71.5 [Si(OSi)<sub>2</sub>], -79.9 [Si(OSi)<sub>3</sub>]; FTIR (ATR):  $\nu = 3064$  [w;  $\nu_{\text{stretch}}(\text{=CH}_2)$ ], 3024 [w;  $\nu_{\text{stretch}}(\text{=CH})$ ], 2984 (w), 2958 (w), 2845 [w;  $\nu_{\text{stretch}}(\text{OCH}_3)$ ], 1970 [w;  $\nu_{\text{stretch}}(\text{C=C=C})$ ], 1939 [w;  $\nu_{\text{stretch}}(\text{C=C=C})$ ], 1601 (m), 1563 [m;  $\nu_{\text{as}}(\text{OCO})$ ], 1431 [m;  $\nu_{\text{s}}(\text{OCO})$ ], 1410 (m), 1277 (m), 1220 (m), 1195 [m;  $\nu_{\text{stretch}}(\text{SiOSi})$ ], 1108 [m;  $\nu_{\text{stretch}}(\text{SiOCH}_3)$ ], 1031 [s;  $\nu_{\text{stretch}}(\text{SiOSi})$ ], 963 [s;  $\nu_{\text{stretch}}(\text{SiOH})$ ], 807 [s;  $\nu_{\text{bend}}(\text{SiO})$ ], 755 (s), 691  $\text{cm}^{-1}$  (s).

### Synthesis of the $\text{Zr}_6/\text{MPTMS}/\text{BPO}$ Copolymer

#### ( $\text{Zr} : \text{Si}$ molar ratio 1 : 10)

An initial suspension of  $[\text{Zr}_6\text{O}_4(\text{OH})_4(\text{O}_2\text{CCH}_2\text{C}\equiv\text{CH})_{12}]$  (0.270 g) in anhydrous THF (1.2 mL) was stirred at room temperature for a few minutes. MPTMS (2.0 mL) and BPO (1 wt % of MPTMS) were added and the mixture was stirred at room temperature for 2 h and  $1/2$ , or until a yellow clear solution was obtained.

For the preparation of the bulk specimen, the previous solution was left to evaporate to dryness, leaving a yellow transparent xerogel ( $\text{Zr}_6/\text{MPTMS}/\text{BPO}$ ). The sample was then heated at 90°C for 30 min. A cylindrical sample of length 4.81 mm and diameter 6.00 mm was produced. DMS analysis — after the 1st run:  $3.97 \times 6.22$  mm; 2nd run:  $3.71 \times 6.04$  mm; 3rd run:

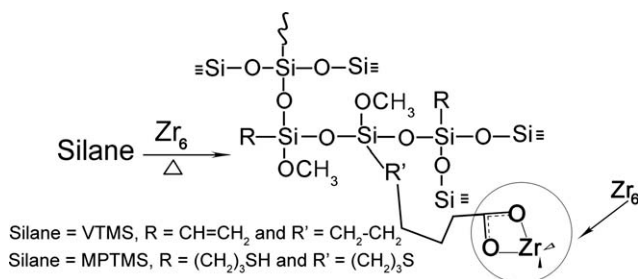


**Figure 1.** Synthesis of the Zr<sub>6</sub>/MPTMS/BPO and Zr<sub>6</sub>/VTMS/BPO copolymer prepared with benzyl peroxide (BPO) as radical initiator. Schematic example of the type of bonds formed in the copolymers.

3.53 × 5.78 mm; 4th run: 3.51 × 5.53 mm; 5th run: 3.45 × 5.52 mm; 6th run: 3.48 × 5.40 mm.

<sup>1</sup>H NMR (400 MHz, δ): 3.4, 2.5, 1.5; <sup>13</sup>C NMR (100 MHz, δ): 51.3 (OCH<sub>3</sub>), 28.6 (CH<sub>2</sub>CH<sub>2</sub>SH and CH<sub>2</sub>SH), 13.2 (SiCH<sub>2</sub>); <sup>29</sup>Si NMR (79 MHz, δ): -49.5 (Si(OSi)), -57.8 (Si(OSi)<sub>2</sub>), -66.8 (Si(OSi)<sub>3</sub>); FTIR (ATR): ν = 3300 (w; ν<sub>stretch</sub>(≡CH)), 2958 (w), 2931 (m), 2888 (w), 2858 [w; ν<sub>stretch</sub>(OCH<sub>3</sub>)], 2798 (w), 2556 [w; ν<sub>stretch</sub>(SH)], 1593 (m), 1526 [w; ν<sub>as</sub>(OCO)], 1427 [w; ν<sub>s</sub>(OCO)], 1407 (m), 1344 (w), 1304 (w), 1260 (m), 1241 (m), 1181 [m; ν<sub>stretch</sub>(SiOSi)], 1097 [m, ν<sub>stretch</sub>(SiOCH<sub>3</sub>)], 1001 [s; ν<sub>stretch</sub>(SiOSi)], 922 (s), 869 (s), 796 [s; ν<sub>bend</sub>(SiO)], 689 cm<sup>-1</sup> (s).

## RESULTS AND DISCUSSION

The 3-butoxate-substituted zirconium-oxocluster [Zr<sub>6</sub>O<sub>4</sub>(O-H)<sub>4</sub>(O<sub>2</sub>CCH<sub>2</sub>C≡CH)<sub>12</sub>] (Zr<sub>6</sub>) was synthesized by the addition of Zr(OPr<sup>n</sup>)<sub>4</sub> in *n*-propanol to 3-butyric acid.<sup>17</sup> The *i/o* hybrid copolymers of Zr<sub>6</sub> with vinyltrimetoxysilane (VTMS) or MPTMS were prepared through a sol-gel process, with benzyl peroxide (BPO) as radical initiator and a Zr to Si molar ratio of 1–10. From FTIR and NMR characterization (discussed in more detail later), it was observed that after polymerization, not all the alkyl chains of the siloxanes were reacted; even when all the triple bonds of the alkynes were reacted, some of the thiol or vinyl groups of the siloxanes remained “free” in the copolymers (see Figure 1). Since the bulk materials were well formed it is possible to imagine a chemical modification or further reaction of the “free” groups to add functionality/specific properties to the copolymers. Possible examples could be the use of the thiol groups for the removal of metal ions,<sup>18–23</sup> as precursors of sulfonic acid moieties to use in catalysis or wettability,<sup>24,25</sup> or as groups to give the material stimuli-response properties.<sup>26,27</sup>

The polymerization process was studied through DSC measurements on the xerogels obtained after evaporation of the solvent (Figure 2), in the range 40–200°C. Non reversible exothermic events, associated with a polymerization, were recorded for both copolymers (line A' and B' in comparison with A and B). The polymerization of Zr<sub>6</sub>/MPTMS/BPO, Line A, started around 114°C. The total enthalpy change was 30 J g<sup>-1</sup>, accompanied by a sample mass loss of -2.5%. The polymerization of Zr<sub>6</sub>/VTMS/BPO, Line B, started around 105°C and continued with a second polymerization event at 152°C. The total enthalpy

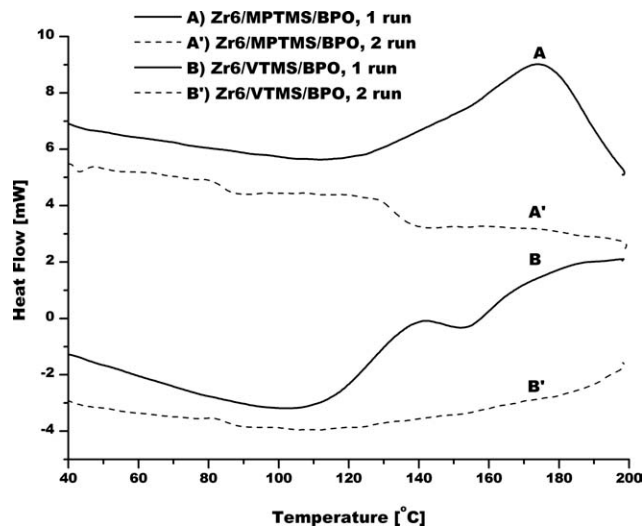


**Figure 2.** DSC analysis of the xerogels (A) Zr<sub>6</sub>/MPTMS/BPO, 1st run; (A') Zr<sub>6</sub>/MPTMS/BPO, 2nd run; (B) Zr<sub>6</sub>/VTMS/BPO, 1st run; and (B') Zr<sub>6</sub>/VTMS/BPO, 2nd run. The analysis was performed from 30° to 200°C in nitrogen with a heating rate of 10°C/min.

change was 61 J g<sup>-1</sup>, with a sample mass loss of -8.5%. The second polymerization event was in accord with a polymerization of the more hindered alkynyl groups bound to the zirconium. It was not evident in the case of the Zr<sub>6</sub>/MPTMS/BPO copolymer because of the higher mobility of the 3-mercaptopropyl chain. The second DSC runs (Figure 2, A' and B') no longer showed the exothermic events and had a mass loss for Zr<sub>6</sub>/MPTMS/BPO and Zr<sub>6</sub>/VTMS/BPO of -0.5% and -1.2%.

The thermo-mechanical properties of the Zr<sub>6</sub>/VTMS/BPO and Zr<sub>6</sub>/MPTMS/BPO copolymers were determined by measuring the shear storage (*G'*) and loss (*G''*) moduli and the tan δ of the materials in the range of 30–300°C, by dynamic mechanical spectroscopy (DMS; Figures 3 and 4). From the tan δ curves of the two copolymers, two small glass transitions were visible; for the Zr<sub>6</sub>/VTMS/BPO at about 70°C, and for Zr<sub>6</sub>/MPTMS/BPO at

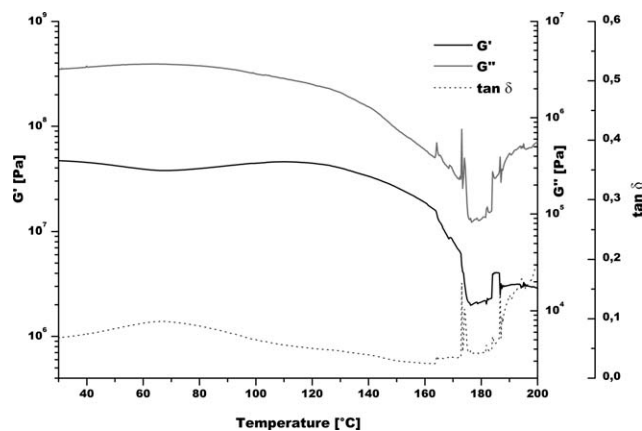


**Figure 3.** *G'*, *G''*, and tan δ curves of the 1st DMS analysis of the Zr<sub>6</sub>/VTMS/BPO copolymer. The analysis was performed in shear mode (oscillation frequency of 1 Hz, force of 1000 mN) from 30°C to 200°C with a heating rate of 2°C/min.

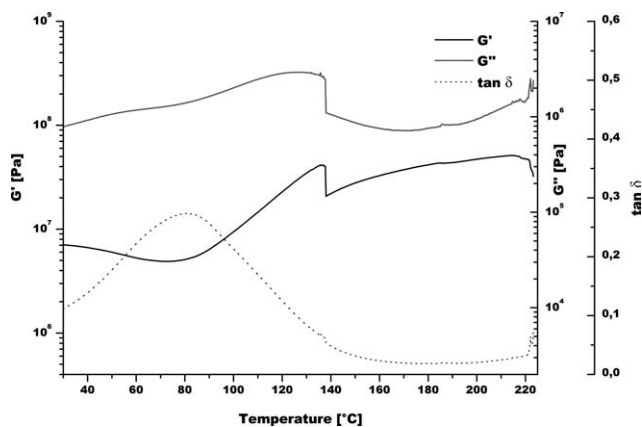


**Figure 4.**  $G'$ ,  $G''$ , and  $\tan \delta$  curves of the 1st DMS of the  $Zr_6$ /MPTMS/BPO copolymer. The analysis was performed in shear mode (oscillation frequency of 1 Hz, force of 1000 mN) from 30°C to 200°C with a heating rate of 2°C/min.

about 80°C. The non-correspondence of the  $\tan \delta$  plots with the corresponding  $G'$  plots, at these temperatures, showed that the glass transitions involved only a part of the materials. For both copolymers, the increase of the  $G'$  curve after the glass transitions was associated with a polymerization involving the C—C multiple bonds. Then, in the case of the  $Zr_6$ /VTMS/BPO,  $G'$  increased constantly until there was a sharp drop corresponding to a second glass-transition temperature ( $T_{gG'} = 173^\circ\text{C}$ ) involving, in this case, the whole material. The first DMS run of both copolymers was interrupted by the shrinkage of the specimens around 200°C. The mass loss was for  $Zr_6$ /MPTMS/BPO and  $Zr_6$ /VTMS/BPO of 7% and 13% and the solid shrinkage 3% and 13%. This shrinkage was attributed to the high reticulation of the copolymers set by the 3-butyrate ligand (as shown in the DSC). While the  $Zr_6$ /MPTMS/BPO specimen was observed to undergo a flattening in response to the applied force, the  $Zr_6$ /VTMS/BPO specimen conserved its shape.

The thermal stability of the copolymers in the first DMS runs was explained by the presence of the Si—O—Si bonds, which formed during the sol-gel preparation of the copolymers through the condensation of the silanes.

The  $Zr_6$ /VTMS/BPO copolymer showed an increase in  $G'$  and  $T_{gG'}$  values in the second DMS run in comparison with the first run ( $G'_{\max} = 140$  MPa,  $T_{gG'} = 238^\circ\text{C}$ ) (Figure 5), though the specimen recovered after the analysis was so fragile that the ends crumbled. In the case of the  $Zr_6$ /MPTMS/BPO copolymer, the specimen maintained its structure over six DMS runs. Subsequent DMS runs for  $Zr_6$ /MPTMS/BPO showed a higher  $G'$  ( $G'_{\max} = 228$  MPa) and  $T_{gG'}$  (up to 300°C), which might imply further reticulation inside the copolymer through the formation of S—S bonds. The slow fade of the  $G'$  value after the 3rd run (Figure 5) and the higher mobility of the copolymer acquired after 60°C were attributed to the rupture of the S—S bonds and the oxidation of the sulfur to  $\text{SO}_2/\text{SO}_3$ , as the run was performed under air.

The bulk materials produced after polymerization were transparent with a slight yellow tint. It was noticed that after having

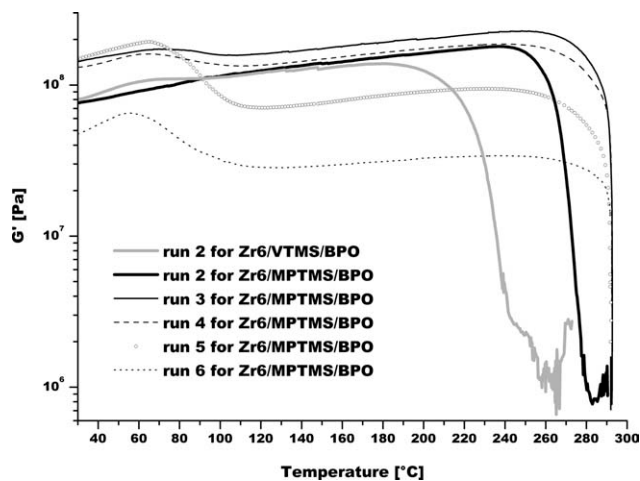


**Figure 5.**  $G'$  curves of the 2nd DMS run of the  $Zr_6$ /VTMS/BPO copolymer and 2nd to 6th DMS runs of the  $Zr_6$ /MPTMS/BPO copolymer. The analysis was performed in shear mode (oscillation frequency of 1 Hz, force of 1000 mN) from 30°C to 300°C with a heating rate of 2°C/min.

been subjected to heating in DSC or DMS (up to 200° or 300°C, respectively), the copolymers darkened slightly, more intense in the case of  $Zr_6$ /VTMS/BPO. Both copolymers were thermally stable.

From FTIR studies, the thiol or vinyl groups of the siloxanes that remained “free” in the copolymers were well visible. The FTIR also showed that in the case of  $Zr_6$ /VTMS/BPO, the polymerization seemed to proceed through the isomerization of the 3-butyrate to the buta-2,3-dienoate (i.e., the alkyne changes into the allene isomer). For  $Zr_6$ /MPTMS/BPO this isomerization step was not detected, probably due to the fast kinetics of the thiol-alkyne polymerization.

FTIR analysis of the  $Zr_6$ /VTMS/BPO copolymer obtained after thermally treating the xerogel at 90°C for 30 min (Figure 6,

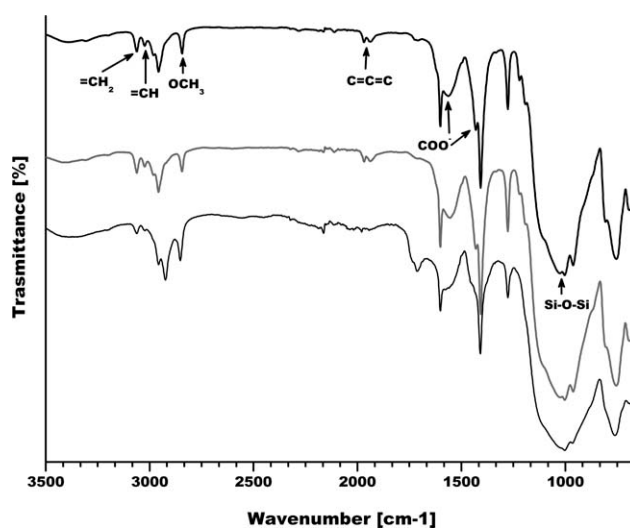


**Figure 6.** FTIR spectrum of the  $Zr_6$ /VTMS/BPO copolymer after heating at: 90°C for 30 min (bold black line); 120°C for 30 min (bold gray line); 120°C over night (black line).

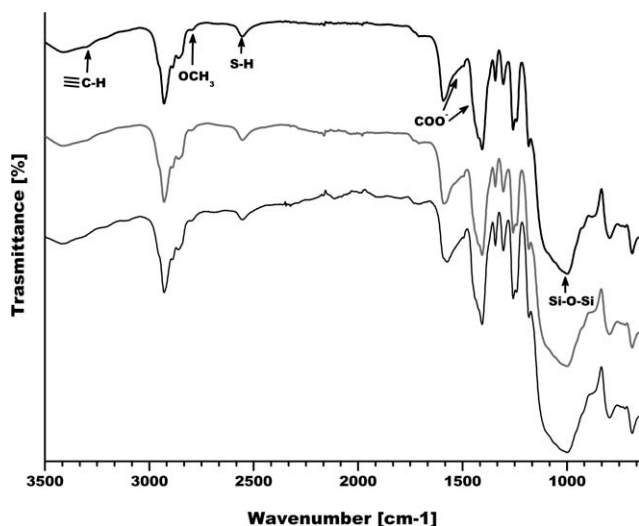


**Figure 7.** FTIR spectrum of the  $Zr_6$ /MPTMS/BPO copolymer after heating at: 90°C for 30 min (bold black line); 120°C for 30 min (bold gray line); 120°C over night (black line).

black bold line) showed that a siloxane chain was formed, evidenced by the reduced  $OCH_3$  stretching at  $2845\text{ cm}^{-1}$  and the appearance of the  $Si-O$  peak at  $1031\text{ cm}^{-1}$ . The structure of the zirconium-oxocluster was assumed to remain stable after polymerization since its characteristic peaks, such as the  $O=C-O^-$  asymmetric and symmetric stretching at  $1563\text{ cm}^{-1}$  and  $1431\text{ cm}^{-1}$ , were preserved. The two  $C=C=C$  stretching bands of the allene at  $1970$  and  $1939\text{ cm}^{-1}$  and the  $=CH_2$  and  $=CH$  stretching of the vinyl group of the siloxane at  $3064$  and  $3024\text{ cm}^{-1}$  remained visible even after heating the copolymer at  $120^\circ\text{C}$  for 30 min (Figure 6, gray line). Heating at  $120^\circ\text{C}$  for one night led to the disappearance of the  $C=C=C$  stretching bands and only a 2% decrease of the  $=CH_2$  stretching band (Figure 6, black line).

Similarly, the FTIR analysis of the  $Zr_6$ /MPTMS/BPO copolymer (Figure 7, black bold line) showed that though siloxane chains were formed (broad  $Si-O$  band at  $1001\text{ cm}^{-1}$  and residual  $OCH_3$  stretching band at  $2858\text{ cm}^{-1}$ ), all the zirconium-oxocluster ( $1526$  and  $1427\text{ cm}^{-1}$ ) features were preserved along with the peaks of the stretching of residual  $\equiv C-H$  and  $S-H$  bonds at  $3300$  and  $2556\text{ cm}^{-1}$ . Additional heating at  $120^\circ\text{C}$  for 30 min led to the partial disappearance of the triple bond of the alkyne. Heating overnight at  $120^\circ\text{C}$  caused the triple bonds to completely disappear (Figure 7 black lines). However, the  $S-H$  stretching band was still present (with a 10% decrease of the peak) and disappeared from the FTIR spectrum only after heating the sample to  $300^\circ\text{C}$  for six DMS runs (here not reported). The removal of the  $S-H$  groups was consistent with the hypothesis that the  $S-H$  groups react to form  $S-S$  bonds which were responsible for the increased stiffness recorded in the first and second DMS runs, as discussed before. It is important to consider that while under oxidizing conditions thiol groups react to give disulfide bridges, under reducing conditions the disulfide bridges can be cleaved to re-generate the thiol groups. A reversible disulfide cross-linking would be an impor-

tant achievement since is at the base of the development of mendable and smart materials.<sup>28–30</sup>

The bulk materials were further characterized by NMR, which confirmed the FTIR observations.  $^{29}\text{Si}$  MAS NMR of both  $Zr_6$ /VTMS/BPO and  $Zr_6$ /MPTMS/BPO copolymers, obtained after polymerization, showed three peaks at  $-62.9$ ,  $-71.5$ ,  $-80.0$ , and  $-49.5$ ,  $-57.8$ ,  $-66.8\text{ ppm}$ , respectively. They correspond to the  $T^1$  [ $\text{RSi}(\text{OSi})(\text{OCH}_3)_2$ ],  $T^2$  [ $\text{RSi}(\text{OSi})_2(\text{OCH}_3)$ ], and  $T^3$  [ $\text{RSi}(\text{OSi})_3$ ] series. No siloxane precursors,  $T^0$  species, were observed. The integrations of the  $T^1$ ,  $T^2$ , and  $T^3$  peaks were about 7%, 53%, 40% for  $Zr_6$ /VTMS/BPO and 8%, 51%, 41% for  $Zr_6$ /MPTMS/BPO. For both copolymers, the DC, determined by calculation of the integration of the  $^{29}\text{Si}$  NMR peaks, was 0.78,<sup>5,31</sup> irrespective of the type of R in the monomers. When a reduced amount of  $Zr_6$  was employed (Zr to Si ratio of 1 to 40), the percentages of the  $T^2$  and  $T^3$  units were similar ( $T^1$  4%,  $T^2$  49%,  $T^3$  47%, DC = 0.81) because the condensation among silanes was predominant over the radical polymerization.

In the  $^{13}\text{C}$  MAS spectrum of  $Zr_6$ /VTMS/BPO (Figure 8, lower spectrum), the  $=CH_2$  and  $=CH$  peaks of the vinyl groups of the siloxanes at  $128.0$  and  $133.8\text{ ppm}$  were predominant and a small peak at  $47.8\text{ ppm}$  was assigned to the carbon of the methoxy groups. The peaks of the  $Zr_6$  were also visible ( $214.3$ ,  $172.0$ ,  $88.6$ ,  $75.9$ ,  $69.6$ ,  $25.8\text{ ppm}$ ), suggesting that the zirconium-oxocluster structure had not been changed. The integration of these peaks confirmed that only a small amount of 3-butynoate,  $69.6\text{ ppm}$  ( $\equiv\text{CH}$ ), was present while the buta-2,3-dienoate form was prevalent ( $\text{CH}_2-\text{C}=\text{C}=\text{C}$  at  $88.6\text{ ppm}$ ). New peaks at  $223.0$  and  $217.7\text{ ppm}$ , not present in the  $^{13}\text{C}$  MAS spectrum of the sole  $Zr_6$  (Figure 8, upper spectrum), were assigned to the  $\text{C}=\text{C}=\text{C}$  of two non-equivalent buta-2,3-dienoate ligands, while new peaks at  $53.5$ ,  $39.6$ , and  $17.8\text{ ppm}$  were

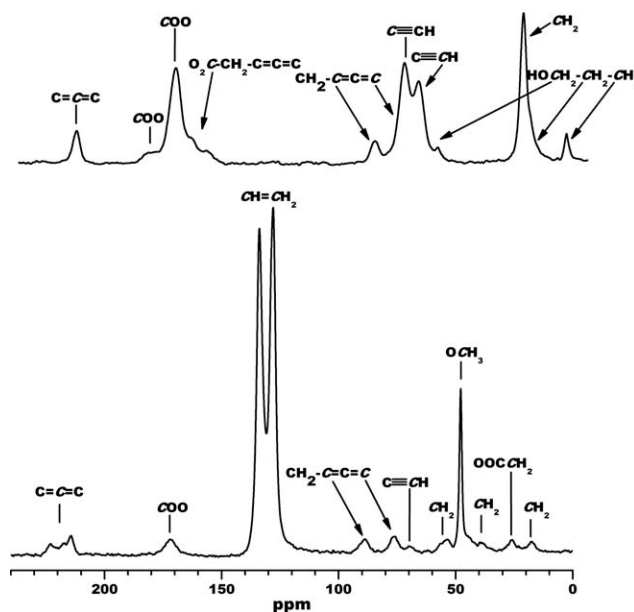


**Figure 8.**  $^{13}\text{C}$  MAS spectrum of the  $[Zr_6O_4(\text{OH})_4(\text{OOCCH}_2\text{CCH})_{12}]$  ( $Zr_6$ ) (upper) and the  $Zr_6$ /VTMS/BPO copolymer (lower).

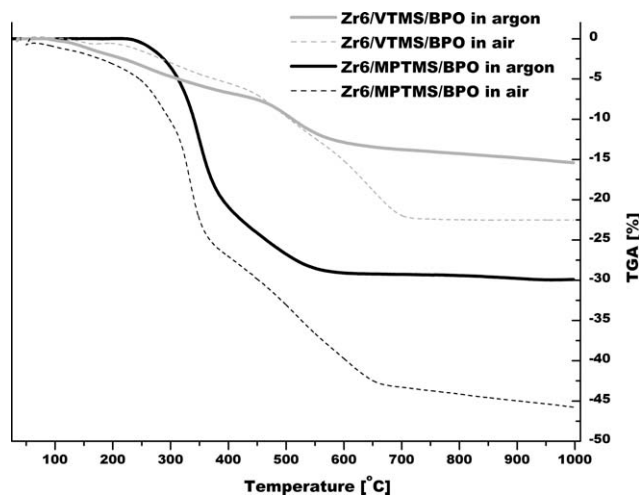


**Figure 9.** TGA analysis of the two copolymers:  $Zr_6/VTMS/BPO$  and  $Zr_6/MPTMS/BPO$ , performed in argon and in air. The analysis was performed from 25° to 1000°C with a heating rate of 10°C/min.

attributed to  $CH_2$  peaks of the saturated organic ligands derived from the alkynes after the polymerization. Unfortunately, in the  $^{13}C$  MAS of  $Zr_6/MPTMS/BPO$ , only the peaks of the MPTMS could be assigned since the peaks of the  $Zr_6$  appeared to be too broad and weak, due to a dilution effect.

The thermal resistance of the materials were analyzed through TGA under both air and argon atmospheres (Figure 9). The  $Zr_6/VTMS/BPO$  copolymer showed a continuous low initial mass loss, due to thermal condensation of the methoxy groups; then, at temperatures higher than about 300°C, the depolymerization and combustion started. The condensation of the methoxy groups in the  $Zr_6/VTMS/BPO$  copolymer was probably favored by the short distance among the siloxane groups due to the short carbon chains generated by the vinyl groups. When argon was used, the total mass loss was about 15%. In air, the thermal trend was the same, but the mass loss of combustion was larger for a total mass loss of about 23%. The TGA of the  $Zr_6/MPTMS/BPO$  copolymer showed, in argon, a single decomposition at about 250°C and, in air, two others at 200° and 350°C, attributable to depolymerization/combustion and the oxidation of the sulfur to  $SO_2/SO_3$ .

## CONCLUSIONS

The  $Zr_6/VTMS/BPO$  and  $Zr_6/MPTMS/BPO$  copolymers were synthesized and their properties investigated. The thermo-mechanical studies for the  $Zr_6/VTMS/BPO$  copolymer showed a high storage modulus ( $G'$ ) and high glass transition ( $T_{gG'}$ ) in the first DMS analysis, further improved to a  $G'_{max}$  of 140 MPa (at 180°C) and a  $T_{gG'}$  of 238°C in the second DMS run. More impressive results were obtained with the  $Zr_6/MPTMS/BPO$  copolymer, which reached a  $G'_{max}$  of 228 MPa at 248°C, and a  $T_{gG'}$  of ~290°C after the first DMS run. The copolymer underwent six DMS runs without destruction, conserving a  $T_{gG'}$  of about 300°C.

In addition to the impressive thermo-mechanical properties, the copolymers possess free unreacted functional groups in the alkyl

chain of the siloxanes which could serve as valuable platform for chemical modification or further reactions to add extra functionality in the copolymers. Further investigation of these materials for use as coatings for cellulose is warranted.

## ACKNOWLEDGMENTS

The Provincia Autonoma di Trento, through the grant CE-NA-CO-LI (nanostructured metal oxide and inorganic–organic hybrid coatings for cellulose and lignin, paper and wood, for preservation against fungi and chemical attack and as flame retardant—keywords: cellulose, nanocomposites, coating, lignin).

## REFERENCES

- Gross, S. *J. Mater. Chem.* **2011**, *21*, 15853.
- Gross, S.; Müller, K. *J. Sol-Gel Sci. Technol.* **2011**, *60*, 283.
- Schubert, U. *Chem. Soc. Rev.* **2011**, *40*, 575.
- Di Maggio, R.; Callone, E.; Girardi, F.; Dire, S. *J. Appl. Polym. Sci.* **2012**, *125*, 1713.
- Graziola, F.; Girardi, F.; Di Maggio, R.; Callone, E.; Miorin, E.; Negri, M.; Müller, K.; Gross, S. *Progr. Org. Coat., to appear*.
- Di Maggio, R.; Dire, S.; Callone, E.; Girardi, F.; Kickelbick, G. *Polymer* **2010**, *51*, 832.
- Di Maggio, R.; Dire, S.; Callone, E.; Girardi, F.; Kickelbick, G. *J. Sol-Gel Sci. Technol.* **2008**, *48*, 168.
- Lowe, A. B.; Hoyle, C. E.; Bowman, C. N. *J. Mater. Chem.* **2010**, *20*, 4745.
- Hoogenboom, R. *Angew. Chem., Int. Ed.* **2010**, *49*, 3415.
- Fairbanks, B. D.; Scott, T. F.; Kloxin, C. J.; Anseth, K. S.; Bowman, C. N. *Macromolecules* **2009**, *42*, 211.
- Hoyle, C. E.; Lowe, A. B.; Bowman, C. N. *Chem. Soc. Rev.* **2010**, *39*, 1355.
- Hoyle, C. E.; Lee, T.Y.; Roper, T. J. *Polym. Sci. Part A: Polym. Chem.* **2004**, *42*, 5301.
- Heitner, C. In *Photochemistry of Lignocellulosic Materials*, Heitner, C., Scaiano, J. C., Eds.; ACS Symposium Series 531: Washington, DC, **1993**; *8*, 192.
- Cook, C. M.; Pan, X.; Ragauskas, A. J. *J. Wood Chem. Technol.* **1996**, *16*, 327.
- Xi, F.; Barclay, L. R. *Can. J. Chem.* **1998**, *76*, 171.
- Wan, J. K. S.; Depew, M. C. *Res. Chem. Intermed.* **1996**, *22*, 241.
- Maggini, S.; Girardi, F.; Müller, K.; Di Maggio, R. *J. Appl. Polym. Sci.* **2012**, *124*, 2110.
- Zhang, W.-H.; Zhang, X.; Zhang, L.; Schroeder, F.; Harish, P.; Hermes, S.; Shi, J.; Fischer, R. A. *J. Mater. Chem.* **2007**, *17*, 4320.
- Zhang, Z.; Dai, S.; Fan, X.; Blom, D. A.; Pennycook, S. J.; Wei, Y. *J. Phys. Chem. B* **2001**, *105*, 6755.
- Kang, T.; Park, Y.; Yi, J. *Ind. Eng. Chem. Res.* **2004**, *43*, 1478.
- Mercier, L.; Pinnavaia, T. J. *Adv. Mater.* **1997**, *9*, 500.

22. Feng, X.; Fryxel, G. E.; Wang, L.-Q.; Kim, A. Y.; Liu, J.; Kemner, K. M. *Science* **1997**, *276*, 923.
23. Liu, A. M.; Hidajat, K.; Kawi, S.; Zhao, D. Y. *Chem. Commun.* **2000**, 1145.
24. Van Rhijin, W. M.; De Vos, D. E.; Sels, B. F.; Bossaert, W. D.; Jacobs, P. A. *Chem. Commun.* **1998**, 317.
25. Oh, Y.-K.; Hong, L.-Y.; Asthana, Y.; Kim, D.-P. *J. Ind. Eng. Chem.* **2006**, *12*, 911.
26. Roy, D.; Cambre, J. N.; Sumerlin, B. S. *Prog. Polym. Sci.* **2010**, *35*, 278.
27. Bencini, M.; Ranucci, E.; Ferruti, P.; Manfredi, A. *Macromol. Rapid Commun.* **2006**, *27*, 1060.
28. Bergman, S. D.; Wudl, F. *J. Mater. Chem.* **2008**, *18*, 41.
29. Milanesi, L.; Hunter, C. A.; Tzokova, N.; Waltho, J. P.; Tomas, S. *Chem. Eur. J.* **2011**, *17*, 9753.
30. Yoon, J. A.; Kamada, J.; Koynov, K.; Mohin, J.; Nicolaÿ, R.; Zhang, Y.; Balazs, A. C.; Kowalewski, T.; Matyjaszewski, K. *Macromolecules* **2012**, *45*, 142.
31. Dong, H.; Lee, M.; Thomas, R. D.; Zhang, Z.; Reidy, R. F.; Mueller, D. W. *J. Sol-Gel Sci. Technol.* **2003**, *28*, 5.